6-1-2012

3D Sonar Measurements in Wakes of Ships of Opportunity

Alexander Soloviev
Nova Southeastern University, soloviev@nova.edu

Christopher Maingot
Nova Southeastern University

Mike Agor
CodaOctopus Products, Inc.

Lou Nash
Measutronics Corporation

Keith Dixon
Measutronics Corporation

NSUWorks Citation
Alexander Soloviev, Christopher Maingot, Mike Agor, Lou Nash, and Keith Dixon. 2012. 3D Sonar Measurements in Wakes of Ships of Opportunity .Journal of Atmospheric and Oceanic Technology , (6) : 880 -886. https://nsuworks.nova.edu/occ_facarticles/620.

3D Sonar Measurements in Wakes of Ships of Opportunity

ALEXANDER SOLOVIEV AND CHRISTOPHER MAINGOT

Oceanographic Center, Nova Southeastern University, Dania Beach, Florida

MIKE AGOR

CodaOctopus Products, Inc., Lakeland, Florida

LOU NASH AND KEITH DIXON

Measutronics Corporation, Lakeland, Florida

(Manuscript received 15 July 2011, in final form 19 January 2012)

ABSTRACT

The aim of this work is to test the potential capabilities of 3D sonar technology for studying small-scale processes in the near-surface layer of the ocean, using the centerline wake of ships of opportunity as the object of study. The first tests conducted in Tampa Bay, Florida, with the 3D sonar have demonstrated the ability of this technology to observe the shape of the centerline wake in great detail starting from centimeter scale, using air bubbles as a proxy. An advantage of the 3D sonar technology is that it allows quantitative estimates of the ship wake geometry, which presents new opportunities for validation of hydrodynamic models of the ship wake. Three-dimensional sonar is also a potentially useful tool for studies of air-bubble dynamics and turbulence in breaking surface waves.

1. Introduction

The problem of ship and ship wake detection from space using synthetic aperture radar (SAR) has attracted attention since the launch of the National Aeronautics and Space Administration (NASA) *Seasat* satellite in 1978 (Fu and Holt 1982; Peltzer et al. 1992; Reed and Milgram 2002). Monitoring of ships and ship wakes from satellites is a useful tool for fishing and pollution control, navigational safety, and global security (Eldhuset 1996; Greidanus and Kourti 2006).

The problem of ship detection involves a variety of topics including ship and ship wake hydrodynamics, wind-wave conditions, surface films, radar imaging, image processing, and pattern recognition (Hyman 1999; Benilov et al. 2000; Reed and Milgram 2002; Crisp 2004; Zilman et al. 2004; Vachon 2006; Soomere 2007; Soloviev et al. 2008). A typical ship wake consists of a bow Kelvin wave, stern Kelvin wave, transverse Kelvin wave, centerline wake, and a turbulent region adjacent to the ship (Pichel et al. 2004). The centerline ship wake usually appears in SAR images as a dark scar. The dark appearance of the centerline wake is associated with the reduction of surface roughness due to the suppression of short (Bragg scattering) surface waves by surfactants, wave–current interactions, and turbulence in the wake. The centerline wake can sometimes be traced for tens of kilometers behind the moving ship (Fig. 1a). In some cases, however, the wake is not prominent in SAR (Fig. 1b). The visibility of ship wakes in SAR depends on several factors, including parameters of antenna, polarization, sea state, and wake hydrodynamics (see, e.g., Reed and Milgram 2002).

Recent advances in satellite technology have improved the capabilities of SAR for identifying sea surface features including ships and ship wakes (Brusch et al. 2011; Soloviev et al. 2010). In addition to SAR, infrared and optical imaging has been implemented in ship wake studies both in the field and laboratory (Garrett and Smith 1984; Munk et al. 1987; Brown et al. 1989; Zheng et al. 2001; Gilman et al. 2011; Voropayev et al. 2011, manuscript submitted to *J. Fluid Mech.*).

Hydrodynamic models of the centerline wake attuned to remote sensing techniques provide a new insight into the problem of ship and ship wake detection from space (Fujimura et al. 2010, 2011). These models, however,

Corresponding author address: Alex Soloviev, 8000 North Ocean Drive, Dania Beach, FL 33004.
E-mail: soloviev@nova.edu

DOI: 10.1175/JTECH-D-11-00120.1

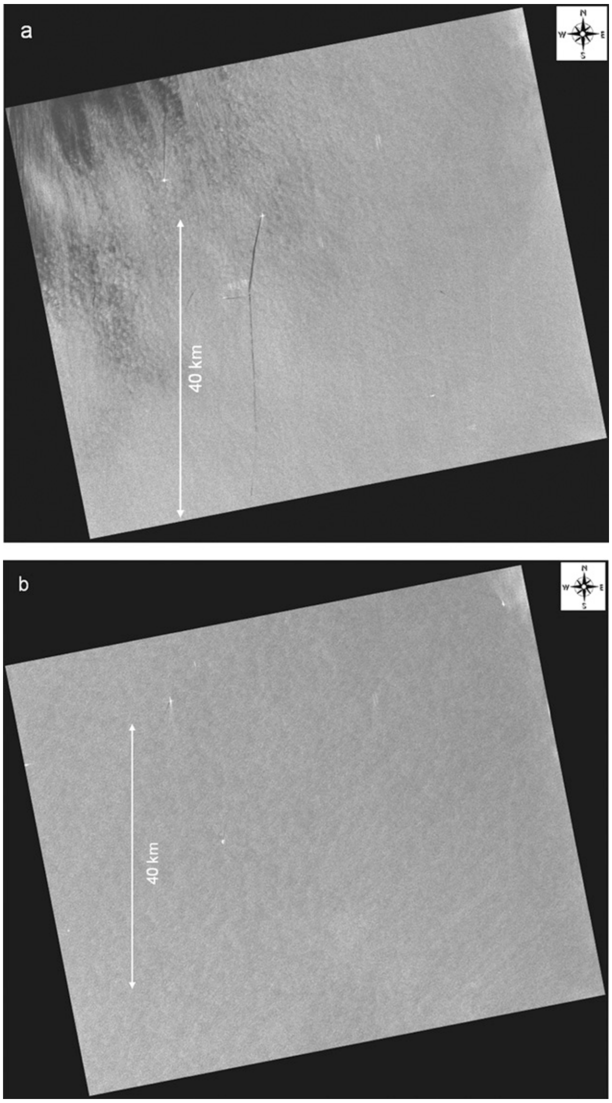

FIG. 1. ALOS PALSAR images taken in the Straits of Florida with (a) prominent and (b) almost invisible wakes behind moving ships.

require validation with in situ measurements. Unfortunately, direct measurement of the velocity field in far wakes with conventional current-measuring technologies is difficult because of the relatively small velocity magnitudes and significant distortions from the orbital velocities of surface waves. One approach to validating these numerical models is through the use of sonar systems to provide an underwater view of the wake.

The presence of bubbles within the wake allow for imaging of the wake with sonar, which responds to a certain bubble size depending on the sonar frequency (Weber et al. 2005). Bubbles within the wake are also believed to be an important factor in the visibility of the ship wake in SAR because of the scavenging of surfactants and transporting them to the sea surface. The surfactants suppress short gravity capillary waves, which makes the wake visible in SAR (Peltzer et al. 1992). Soloviev et al. (2010) reported a case study that observed a correlation between the visibility of the centerline ship wake in SAR and in sonar, which provides additional evidence of the role of bubbles in remote sensing of ship wakes. This correlation, however, may vanish (e.g., under strong wind speed conditions).

In this paper we present the results of ship wake imaging with 3D sonar using the shape of the air bubble clouds as a proxy for the turbulent wake. In section 2, we provide a brief description of the 3D sonar technology and its application for measurements in ship wakes. Section 3 is a comparison of our results to other available laboratory and field data and numerical models on the 3D structure of the centerline ship wake. Section 4 summarizes the main results of this work.

2. 3D sonar and measurements in ship wakes

For tests in the wakes of ships of opportunity, we have employed a real-time 3D imaging system, CodaOctopus Echoscope-UIS (Underwater Inspection System). The sonar has a working frequency of 375 kHz with a 128 × 128 (16 384) array of beams, which provide an angular coverage of 50° × 50° and a beam spacing of 0.39°. The maximum range is 150 m with a range resolution of 3 cm and a ping rate of 12 Hz.

The 3D aspect allows high-resolution visualization to be performed from multiple perspectives (the so-called mosaic view). Three-dimensional images are formed through combining multiple 2D fragments taken from different angles due to the motion of the object with respect to the sonar. The addition of an attitude and positioning system allows the data to be located accurately in 3D space and referenced to the earth's coordinate system. Depth scales are referenced to zero mean sea level, as reported by the GPS. Note that the GPS level may slightly deviate from the actual sea level (Fraczek 2003). To determine the 3D shape of the wake, we have used the edge detection mode of the sonar.

The tests have been conducted in Tampa Bay, Florida. The sonar was attached to the survey vessel named *A Nickel More* using a retractable mount (Fig. 2). During the tests, local ships were tracked using an automatic information system (AIS). This system allowed us to identify the approaching ships and also record information about speed, heading, length, and other parameters.

Figure 3 demonstrates the sonar data during the passage of a tugboat in the Tampa Bay Port Channel. The survey vessel equipped with the sonar system was moving on an opposite course relative to the tugboat at

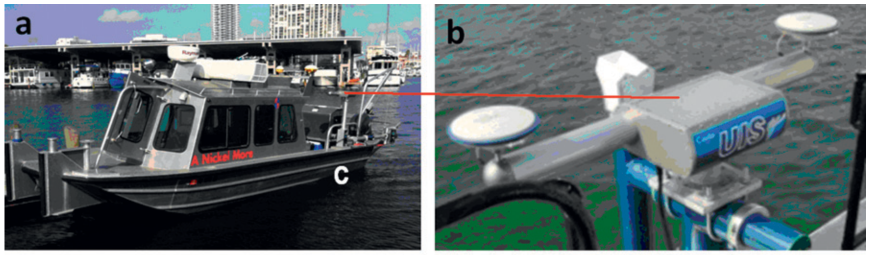

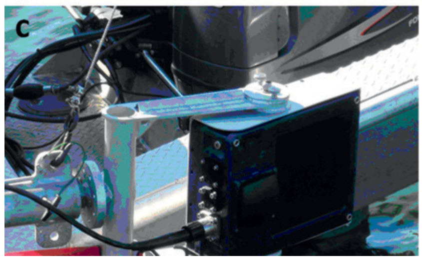

FIG. 2. The CodaOctopus Echoscope-UIS (Underwater Inspection System): (a) the survey vessel *A Nickel More*, (b) the real-time kinematic GPS system and video cameras, and (c) a 3D sonar transducer attached to a retractable mount. The position of the retractable mount holding the sonar transducer during measurements is schematically shown in (a) by the letter C.

approximately 2.6 m s^{-1}. A view of the tugboat from the video camera is shown in Fig. 3a. The sonar image of the tugboat wake is shown in Fig. 3b with surface reflections not removed.

A segment of the tugboat wake visualized with the 3D sonar is shown in more detail in Fig. 3c. This image displays a strong intermittency of the wake shape, while turbulent features are resolved starting from centimeter scale. This segment is shown referenced to the UTM (zone 17N) geographical coordinate system in Fig. 4. Note that surface reflections (as well as signatures of the survey vessel wake) have been removed from Figs. 3c and 4, which was possible due to the three-dimensional aspect of this instrument.

The 3D aspect of the sonar view of the ship wake allows quantitative estimation of the characteristics of the wake segment shown in Fig. 4. For this purpose, we determined the depth of the lower boundary of the wake in 3D space I (see an example in Fig. 7). The relative intermittency of the wake was then estimated using the following formula:

$$F = \sqrt{\overline{(I-\overline{I})^2}}/\overline{I}, \qquad (1)$$

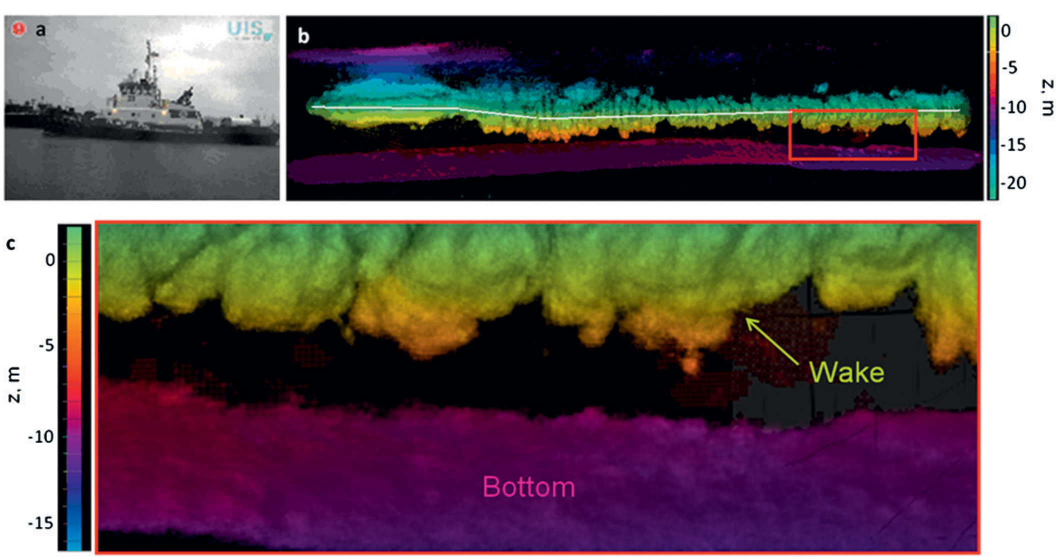

FIG. 3. (a) Snapshot of the tugboat taken from the video and (b) its hull surrounded by the bubble curtain and wake in 3D sonar, with surface reflections. Position of the sea surface is indicated by the white line. The image above the white line, including a purple-blue color above the ship hull, is an artifact due to surface reflections. The red box indicates the area of (c), the enlarged view of the wake with surface reflections removed. Color scales are provided as depth in meters relative to mean sea level. In this color scale, the ocean bottom appears in a purple color.

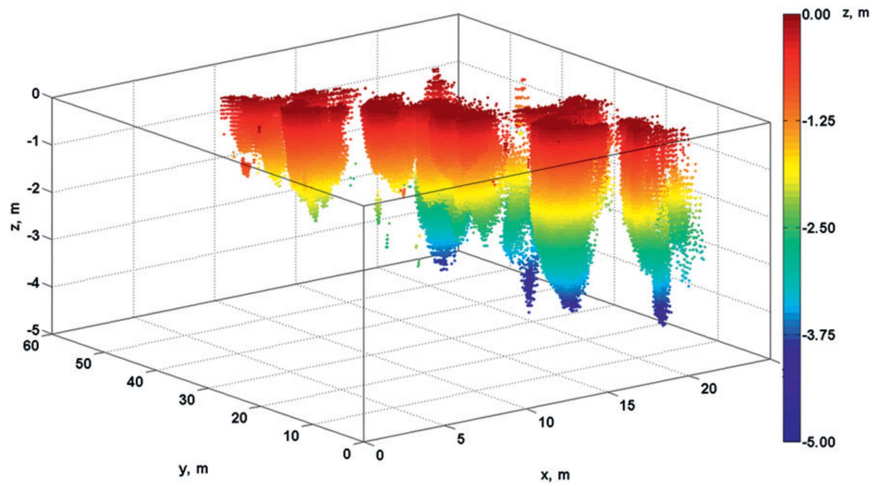

FIG. 4. Segment of the tugboat wake shown in Fig. 3c, plotted in UTM Zone 17N geographical coordinated system with the origin (0, 0) corresponding to location (357646.4756, 3089125.2892). Color scales are provided as depth in meters relative to mean sea level.

where the bar denotes averaging along the ship wake. For this example, the relative intermittency of the wake was $F = 0.38$. This is a simple statistical parameter, which can be useful for validation of numerical models of ship wakes.

A more sophisticated approach may include geometrical properties of boundaries, such as fractal dimensions, which provide clues to the distribution of physical scales in turbulent flows (Sreenivasan et al. 1989; Catrakis 2000). The power spectral density of turbulence can be related to the image fractal dimension (Voss 1988; Meneveau and Sreenivasan 1991). An effective method for evaluating the fractal dimension from images of turbulent clouds has been developed by Zubair and Catrakis (2009). This method is applicable to the analysis of CodaOctopus Echoscope sonar images due the capability of this 3D sonar to produce quantitative measurements of length scales. A method similar to the particle imaging velocimetry (PIV), utilizing the 3D sonar imagery of the bubble cloud boundary, may also be developed in the future for extraction of three-dimensional vector fields. These approaches can also be useful to measure turbulence in breaking wind waves.

Figure 5 shows a snapshot taken from the video record of the cargo ship *Alert* above the water surface with synchronous 3D sonar image below the water surface. Data from the AIS for this vessel give a length of 128 m, a beam of 21 m, a draft of 7.3 m, and a heading of 85° at 5.8 m s^{-1} during the time of the survey. This cargo ship has a bulbous bow. For this example, we can trace the origin of the bubble curtain around the hull to the bulbous bow breaking wave and bow breaking wave.

Figure 6 shows the ship stern and wakes produced by the hull and propeller in 2D view. Because of the relatively slow propeller rotation rate, it is possible to see even the propeller on these sonar images.

The side view of the ship wake in mosaic mode is shown in Fig. 7. The ship wake has red/orange color and the bottom blue/green color, which is due to different distances from the sonar. As illustrated in Fig. 7, the mosaic mode allows the possibility of quantitative estimates of the ship wake geometry.

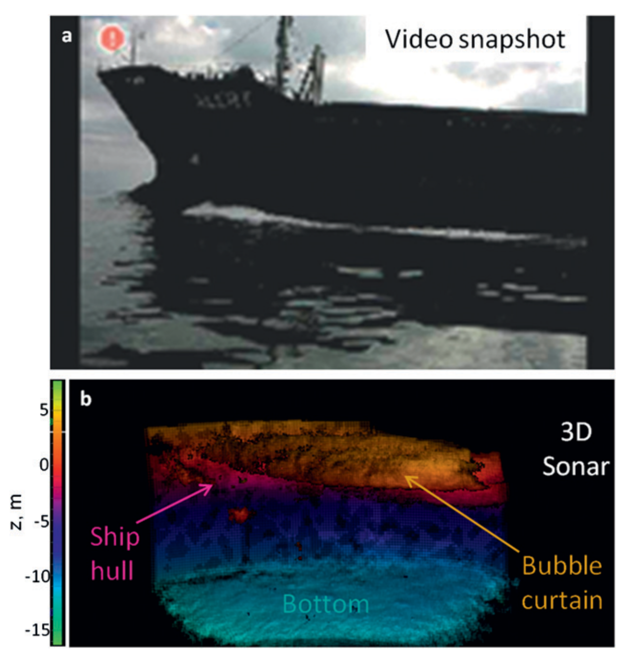

FIG. 5. (a) Snapshot taken from the video of the vessel *Alert*. (b) 3D sonar view of the bubble cloud around *Alert*'s hull. Color scales are provided as depth in meters relative to mean sea level. In this color scale, the ocean bottom appears in a light blue color.

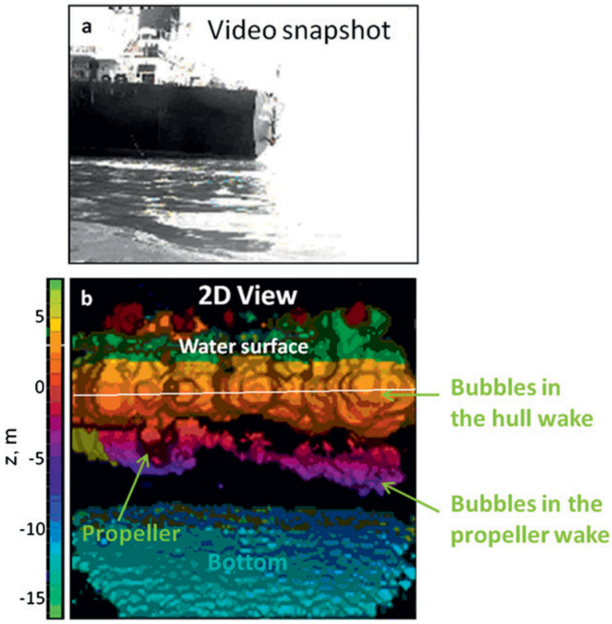

FIG. 6. (a) Snapshot taken from the video of the *Alert*'s stern. (b) Bubbles in *Alert*'s hull and propeller wake (2D view). Color scales are provided as depth in meters relative to mean sea level. In this color scale, the ocean bottom appears in a light blue color. The white line indicates approximate position of the sea surface. The image above this line is formed by surface reflections.

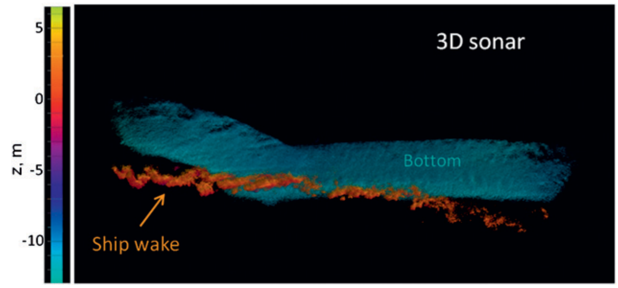

FIG. 8. Aerial view of *Alert*'s wake in 3D. The ship wake has orange color and the bottom a blue color. Color scales are provided as depth in meters relative to mean sea level. In this color scale, the ocean bottom appears in a light blue color.

A bird's-eye view of the *Alert's* wake is shown in Fig. 8. The image in Fig. 8 displays the latter portion of the wake, showing the fragmentation and gradual dissipation of the bubble clouds associated with the wake. Note that in edge detection mode we can only image the outer face of the wake.

3. Discussion

In this section we qualitatively compare the results of the 3D sonar field tests with recent laboratory, field, and modeling results on ship wake dynamics. A review of the previous research for studying ship wakes can be found in Reed and Milgram (2002) and Soloviev et al. (2010).

Voropayev et al. (2011, manuscript submitted to *J. Fluid Mech.*) performed a series of laboratory experiments to study the surface signatures of ship centerline wakes. The experiment was conducted in a tank with temperature stratified water. The wake was created with a self-propelled ship model. An infrared camera registered the signature of the wake in the temperature field on the water surface. The experiments were conducted with distilled water to minimize surfactant effects. From these experiments the temperature signature of the wake revealed meandering, instability, and fragmentation increasing with distance from the model ship. After rescaling, these laboratory results are consistent with the wake observations made with the 3D sonar system in our experiments in Tampa Bay.

Woods Hole Oceanographic Institution (WHOI) conducted an experiment using an airborne Light Detection and Ranging instrument (lidar) to map fluorescent dye released in the centerline wake of Florida Atlantic University's research vessel *R/V Stephan* (Ledwell and Terray 2005). In this experiment, conducted in the Straits of Florida, the airplane flew back and forth over the centerline ship wake, measuring the wake structure with the lidar instrument. Data collected by lidar showed meandering, instability, fragmentation, and dissipation of the ship wake over time. Although the environmental conditions in the Straits of Florida are different from those in Tampa Bay, our results from the 3D sonar experiment in ship wakes are qualitatively consistent with the WHOI dye release experiment.

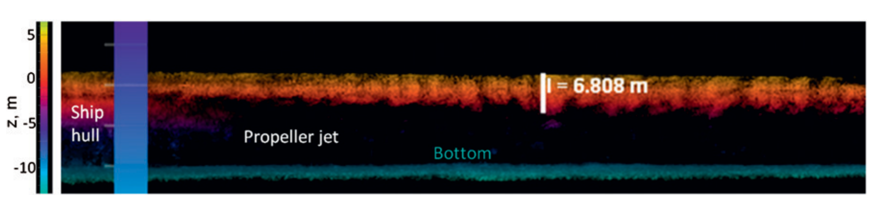

FIG. 7. Wake geometry of the cargo ship *Alert*. Color scales are provided as depth in meters relative to mean sea level. The white vertical segment is to demonstrate the possibility of a quantitative estimate of the wake size in the vertical direction. Note that the large blue bar on the left is a distortion of measurements when the survey boat crossed the *Alert*'s Kelvin wave.

Development of a realistic model for far wakes of ships is still a challenge. The new sonar technology is expected to help with validation of such models. Fujimura et al. (2011) conducted high-resolution numerical experiments with the computational fluid dynamics (CFD) software ANSYS FLUENT on the dynamics of centerline ship wakes in the presence of near-surface stratification and wind stress. The ship wake model was initialized using a model of a ship hull and propellers. The modeling results reveal characteristic features of the centerline wake (meandering, instability, fragmentation, and dissipation). The 3D sonar measurements provide qualitative validation for the modeling results. These measurements can potentially be used for quantitative validation of ship-wake models, for example, using the relative intermittency factor introduced by Eq. (1). However, numerical simulations for the specific ships of opportunity used in the Tampa Bay test are not available.

The abovementioned laboratory, field, and numerical results are qualitatively consistent with our experiments with 3D sonar in wakes of ships of opportunity. The 3D sonar technology greatly enhances the capabilities in studying ship wakes. The application of 3D sonar has provided spatial structure of the ship wake in detail starting from a centimeter scale using air bubbles as a proxy. It should be noted that the air bubbles in the wake may not exactly characterize the velocity field in the wake because of their rising to the surface or dissolution. The bubbles bring surface active materials to the surface, which suppress short gravity capillary waves, thus providing a link between the wake's visibility in sonar and in airborne and spaceborne SAR.

Three-dimensional wake images obtained during our measurements of a large cargo vessel's wake (Figs. 5–8) have elucidated the process of air entrainment by the ship's hull. The air entrainment for this type of hull occurs predominately at the bow of the ship and along the hull sides. The relatively slow revolution rate of the propeller of this ship has also allowed us to visualize the propeller wake in great detail as seen in Fig. 6. Propeller cavitation can be a source of bubbles detected by the sonar in the propeller wake.

Our experiments with 3D sonar have also revealed intermittency in the ship wake similar to that previously observed in the numerical model, laboratory experiments, and field dye release experiment. With the 3D sonar technology, we have been able to explore the features of the wake in the field in three dimensions and in great detail. The mosaic mode allows the possibility of quantitative estimates of the ship wake geometry and visualization of the wake's generation, fragmentation, and dissipation. The 3D sonar technology provides a new insight into ship wake dynamics. These observations are useful for validation of hydrodynamic models, with application to remote sensing of ship wakes. The 3D sonar technology using edge detection of bubble clouds may also provide important insight into the mechanism of surface wave breaking and upper ocean turbulence generation.

4. Conclusions

In this article, we have demonstrated the application of 3D sonar technology to study finescale processes in wakes of ships. Sonar responds to air bubbles in the wake; the bubbles in the wake also contribute to the wake's visibility in SAR by bringing surfactants to the surface and suppressing short (Bragg scattering) gravity capillary waves. The first application of 3D sonar has made the spatial structure of the ship wake observable in great detail starting from a centimeter scale using air bubbles as a proxy. The tests in Tampa Bay, Florida, in wakes of ships of opportunity suggest that 3D sonar technology will be useful for validation of hydrodynamic models with application to remote sensing of ship wakes. The 3D sonar technology may also be helpful in quantifying turbulence in air-bubble clouds, such as breaking surface waves.

Acknowledgments. We thank Jenny Fenton for arranging access to SAR images of ship wakes and Silvia Matt (NSU OC) for discussion of the project results. We acknowledge the Alaska Satellite Facility for providing access to the ALOS PALSAR satellite imagery.

This work was supported by the NSU OC Project "Hydrodynamics and Remote Sensing of Far Wakes of Ships" and by the ONR Award N00014-10-1-0938 "Characterization of Impact of Oceanographic Features on the Electromagnetic Fields in Coastal Waters."

REFERENCES

Benilov, A., G. Bang, A. Safray, and I. Tkachenko, 2000: Ship wake detectability in the ocean turbulent environment. *Proc. 23rd Symp. on Naval Hydrodynamics,* Val de Reuil, France, Office of Naval Research, 687–703.

Brown, E. D., S. Buchsbaum, R. E. Hall, J. P. Penhune, K. F. Schmitt, K. M. Watson, and D. C. Wyatt, 1989: Observations of a nonlinear solitary wavepacket in the Kelvin wave of a ship. *J. Fluid Mech.,* **204,** 263–293.

Brusch, S., S. Lehner, T. Fritz, M. Soccorsi, A. Soloviev, and B. van Schie, 2011: Ship surveillance with TerraSAR-X. *IEEE Trans. Geosci. Remote Sens.,* **49,** 1092–1103.

Catrakis, H. J., 2000: Distribution of scales in turbulence. *Phys. Rev. E,* **62,** 564–578.

Crisp, D. J., 2004: The state-of-the-art in ship detection in synthetic aperture radar imagery. Defence Science and Technology Organisation Information Sciences Laboratory, Australian Department of Defense, DSTO-RR-0272, 116 pp.

Eldhuset, K., 1996: An automatic ship and ship wake detection system for spaceborne SAR images in coastal regions. *IEEE Trans. Geosci. Remote Sens.,* **34,** 1010–1019.

Fraczek, W., 2003: Mean sea level, GPS, and the geoid. *ArcUser,* Summer 2003, ESRI Office, Redlands, CA, 36–41. [Available online at http://www.esri.com/news/arcuser/0703/geoid1of3.html.]

Fu, L. L., and B. Holt, 1982: Seasat views oceans and sea ice with synthetic-aperture radar. Jet Propulsion Laboratory Publication 81-120, 200 pp.

Fujimura, A., A. Soloviev, and V. Kudryavtsev, 2010: Numerical simulation of the wind stress effect on SAR imagery of far wakes of ships. *IEEE Geosci. Remote Sens. Lett.,* **7,** 646–649.

——, S. Matt, A. Soloviev, C. Maingot, S. H. Rhee, 2011: The impact of thermal stratification and wind stress on sea surface features in SAR imagery. *Proc. IGARSS 2011,* Vancouver, BC, Canada, IEEE, 2037–2040.

Garrett, W. D., and P. M. Smith, 1984: Physical and chemical factors affecting the thermal IR imagery of ship wakes. Naval Research Laboratory Memo. Rep. 5376, 24 pp.

Gilman, M., A. Soloviev, and H. Graber, 2011: Study of the far wake of a large ship. *J. Atmos. Oceanic Technol.,* **28,** 720–733.

Greidanus, H., and N. Kourti, 2006. Findings of the DECLIMS project: Detection and classification of marine traffic from space. *Proc. SEASAR 2006*, ESA Publication SP-613, Frascati, Italy, ESA, 25.1.

Hyman, M., 1999: Computation of ship wake flows with free-surface/turbulence interaction. *Proc. 22nd Symp. on Naval Hydrodynamics*, Washington, D.C., Office of Naval Research, 835–847.

Ledwell, J., and G. Terray, 2005: An experiment to dye for: Researchers trace movement of water using airborne laser. *Oceanus,* Vol. 44 (2), Woods Hole Oceanographic Institution. [Available online at http://www.whoi.edu/oceanus/viewArticle.do?id=6858&archives=true.]

Meneveau, C., and K. R. Sreenivasan, 1991: The multifractal nature of turbulent energy dissipation. *J. Fluid Mech.,* **224,** 429–484.

Munk, W. H., P. Scully-Power, and F. Zachariasen, 1987: The Bakerian lecture, 1986: Ships from space. *Proc. Roy. Soc. London,* **412A,** 231–254.

Peltzer, R. D., O. M. Griffin, W. R. Barger, and J. A. C. Kaiser, 1992: High-resolution measurements of surface-active film redistribution in ship wakes. *J. Geophys. Res.,* **97,** 5231–5252.

Pichel, W. G., P. Clemente-Colon, C. C. Wackerman, and K. S. Friedman, 2004: Ship and wake detection. *Synthetic Aperture Radar Marine User's Manual*, C. R. Jackson and J. R. Apel, Eds., NOAA, 277–303.

Reed, A. M., and J. H. Milgram, 2002: Ship wakes and their radar images. *Annu. Rev. Fluid Mech.,* **34,** 469–502.

Soloviev, A., M. Gilman, K. Moore, K. Young, and H. Graber, 2008: Hydrodynamics and remote sensing of far wakes of ships. *SEASAR 2008—The Second Int. Workshop on Advances in SAR Oceanography,* Frascati, Italy, ESA. [Available online at http://earth.esa.int/workshops/seasar2008/participants/187/pres_187_soloviev.pdf.]

——, ——, K. Young, S. Brusch, and S. Lehner, 2010: Sonar measurements in ship wakes simultaneous with TerraSAR-X overpasses. *IEEE Trans. Geosci. Remote Sens.,* **48,** 841–851.

Soomere, T., 2007: Nonlinear components of ship wake waves. *Appl. Mech. Rev.,* **60,** 120–138.

Sreenivasan, K., R. Ramshankar, and C. Meneveau, 1989: Mixing, entrainment and fractal dimensions of surfaces in turbulent flows. *Proc. Roy. Soc. London,* **421A,** 79–108.

Vachon, P. W., 2006: Ship detection in synthetic aperture radar aperture imagery. *Proc. OceanSAR 2006,* St. John's, NL, Canada, Canadian Space Agency [Available online at http://www.oceansar2006.com/papers/82_Vachon_Oceansar2006.pdf.]

Voss, R., 1988: Fractals in nature: From characterization to simulation. *The Science of Fractal Images,* H. Peitgen and D. Saupe, Eds., Springer-Verlag, 21–70.

Weber, T. C., A. P. Lyons, and D. L. Bradley, 2005: An estimate of the gas transfer rate from oceanic bubbles derived from multibeam sonar observations of a ship wake. *J. Geophys. Res.,* **110,** C04005, doi:10.1029/2004JC002666.

Zheng, Q., X.-H. Yan, W. T. Liu, V. Klemas, and D. Sun, 2001: Space shuttle observations of open ocean oil slicks. *Remote Sens. Environ.,* **76,** 49–56.

Zilman, G., A. Zapolski, and M. Marom, 2004: The speed and beam of a ship from its wake's SAR images. *IEEE Trans. Geosci. Remote Sens.,* **42,** 2335–2343.

Zubair, F. R., and H. J. Catrakis, 2009: On separated shear layers and the fractal geometry of turbulent scalar interfaces at large Reynolds numbers. *J. Fluid Mech.,* **624,** 389–411.